Journal of Advanced Research 8 (2017) 607–616

Contents lists available at ScienceDirect

Journal of Advanced Research

journal homepage: www.elsevier.com/locate/jare

Original Article

QbD based approach for optimization of Tenofovir disoproxil fumarate loaded liquid crystal precursor with improved permeability

Sharvil Patil, Chandrashekhar Kadam, Varsha Pokharkar *

Department of Pharmaceutics, Poona College of Pharmacy, Bharati Vidyapeeth University, Erandwane, Pune 411 038, Maharashtra, India

GRAPHICAL ABSTRACT

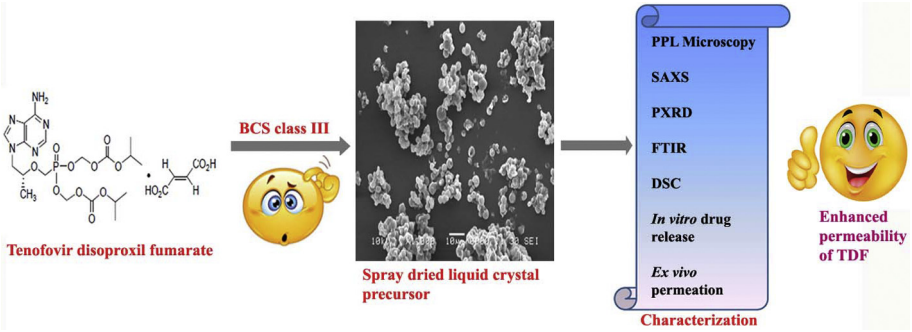

ARTICLE INFO

Article history:
Received 27 April 2017
Revised 27 July 2017
Accepted 28 July 2017
Available online 29 July 2017

Keywords:
Liquid crystal precursor
Glyceryl monooleate
Tenofovir disoproxil fumarate
Quality by design
Permeation flux
Factorial design

ABSTRACT

BCS class III drugs suffer from a drawback of low permeability even though they have high aqueous solubility. The objective of current work was to screen the suitability of glyceryl monooleate (GMO)/Pluronic F127 cubic phase liquid crystals precursors for permeation enhancement and in turn the bioavailability of tenofovir disoproxil fumarate (TDF), a BCS class III drug. Spray-drying method was used for preparation of TDF loaded liquid crystal precursors (LCP) consisting of GMO/Pluronic F127 and lactose monohydrate with an ability to *in situ* transform into stable cubic phases upon hydration. The quality by design (QbD) approach (Factorial design) was used for batch optimization. Spherical TDF loaded LCP as revealed by scanning electron microscopy photographs when hydrated and analyzed by small angle X-ray scattering confirmed formation of cubic phase. Differential scanning calorimetry and X-ray diffraction studies confirmed the molecular dispersion of TDF in polymer matrix and also suggested the conversion of TDF from crystalline to amorphous form. *In vitro* TDF release from prepared LCP showed controlled drug release over a period of 10 h. Further *ex vivo* studies revealed permeation enhancing activity of prepared LCP, which was highest when tested in presence of digestive enzyme extract. Thus, formulation of stable liquid crystal powder precursor can serve as an alternative for designing oral delivery system for drugs with low permeability.

Introduction

Amongst the several routes of drug administration, oral route is the most preferred route as it presents advantages such as convenience, good patient compliance, and low production cost. The physicochemical properties, including solubility and permeability

Peer review under responsibility of Cairo University.

* Corresponding author.
E-mail addresses: varsha.pokharkar@bharatividyapeeth.edu, vbpokharkar@yahoo.co.in (V. Pokharkar).

http://dx.doi.org/10.1016/j.jare.2017.07.005
2090-1232/

are among the factors that govern the absorption of drug molecule into systemic circulation after oral administration. Thence, water soluble drug having good permeability can easily absorbed through GI tract into the systemic circulation when administered orally. As per the biopharmaceutical classification system (BCS), class-III drugs have high solubility and low permeability. Permeation is the rate limiting step in the oral bioavailability of such drugs. Therefore, formulation development of such drugs proposes a major challenge for formulation scientists.

The literature reports various approaches such as the use of bile salts, saponins [1], straight chain fatty acids [2], microemulsion [3], nanoemulsion [4], cyclodextrin inclusion complex [5], chitosan derivatives [6], self-micro-emulsifying drug delivery systems [7], interfacial cohesion and supramolecular assembly of bioadhesive species [8] (including liquid crystals) for permeation enhancement of BCS-III drugs [9]. Additionally, advanced technologies, such as iontophoresis [10], ultrasound [11], microneedles [12,13], electroporation [14], radiofrequency [15], and microporation [16] have been used for enhancing the transdermal permeation of drugs. The reports state the suitability of liquid crystals in bioavailability enhancement of poorly permeable drugs by transdermal route, however their utility in improving oral bioavailability of BCS III drugs remain unexplored.

Glyceryl monooleate (GMO), a polar lipid forms a cubic liquid crystalline phase when comes in contact with water [17]. The cubic phase formed by GMO can deliver drug in sustained manner owing to its highly viscous nature. Slow diffusion or increased residence time of drug molecule in matrix-like system is the possible reason of sustained drug release through cubic phase. Moreover, other properties such as isotropic nature, relative insensitivity to salts and solvents present in intestine, robustness, and resistance to physical degradation makes GMO popular candidate for sustained drug delivery. It is biodegradable and forms oleic acid and glycerol like nontoxic products upon *in vivo* enzymatic degradation by pancreatic lipase [18]. The mesophases of GMO are reported to exhibit bioadhesive property, which in turn improves the chances of gastroretention of the matrices [19]. Moreover, it can solubilize hydrophilic, lipophilic, and amphiphilic drug molecules in its entirely different polarity regions [20]. However, stickiness and stiffness associated with GMO has remained hurdle in formulating it as a drug delivery system. Preparation of powder precursors having ability to *in situ* transform into cubic phase rapidly was attempted by researchers [21,22].

Self-assembling block copolymers have attracted most of the formulation scientists owing to their advantages, such as controlled drug release, bioadhesive nature, and protection of sensitive drug molecules [23]. Pluronic F127 (PF127), a non ionic surfactant, having low toxicity influences the transport of drugs. Additionally, PF127 also influence the permeability of drugs transported across intestine through its P-gp inhibition activity and thus can serve as a carrier of choice for BCS class II, III, and IV drugs [24,25]. Therefore, the objective of current work was to screen the suitability of cubic phase liquid crystals of GMO for permeation enhancement of BCS class III drug upon oral administration. Tenofovir disoproxil fumarate (TDF, BCS class III drug), used as a model drug, having 13.4 mg/mL (25 °C) solubility in water. Thus TDF loaded liquid crystal powder precursors (LCP) containing GMO/PF127 and lactose monohydrate prepared by spray-drying technique. The prepared powder precursors evaluated for percent yield, drug content, particle size, surface topography, phase behavior, physical interaction, *in vitro* drug release, *in vitro* intestinal membrane permeation, and *ex vivo* permeation using everted and non-everted intestinal sac method in presence or absence of digestive enzymes.

Material and methods

Materials

Glyceryl monooleate (Rylo™ MG Pharma 19) was a generous gift from Danisco India Pvt. Ltd. (Gurgaon, Haryana). Pluronic F127 was obtained from Alembic Pharmaceuticals (Mumbai, India). Lactose monohydrate and guaranteed reagent (GR) grade methanol were purchased from Merck Research Lab Pvt. Ltd. (Mumbai, India). Tenofovir disoproxil fumarate (TDF) was supplied as a generous gift from Emcure Pharmaceuticals (Pune, India). All other chemicals used were of analytical grade.

Method

An organic phase was prepared by dissolving GMO, PF127, and TDF in sufficient amount of GR grade methanol (10 mL). Lactose monohydrate was dissolved in water (40 mL) by heating at 40 °C until clear solution was obtained. This preheated aqueous phase was added drop-wise in organic phase with continuous stirring. The prepared solution was then spray-dried using a laboratory-scale spray dryer equipped with a spraying nozzle (Jay Instruments and System Private Limited, Mumbai, India). The spray-drying was carried with following set of conditions: Aspiration-100 mm WC (mm of water column); inlet temperature-100 °C; outlet temperature-45 °C; feed rate-7.5 mL/min, and atomization air pressure-2 kg/cm^2. The solution to be spray-dried was kept under constant stirring and heating on a magnetic stirrer fitted with heater.

QbD approach

Factorial designs were used for optimization of GMO, Pluronic F127, and lactose monohydrate ratio. Different ratios of Pluronic F127 and lactose monohydrate in the range of 0–100% w/w screened keeping the amount of GMO (1 g) and TDF (0.5 g) constant during the preparation of powder precursors. Table 1 shows the levels and factors used for optimization of the batch. The optimized formula for powder precursor consisted of 48.50% w/w GMO, 48.50% w/w lactose monohydrate, and 3% w/w Pluronic F127.

Characterization

Drug content

Accurately weighed 60 mg of TDF loaded LCP was dissolved in appropriate volume of methanol. Solution obtained was filtered through 0.45 μm filter and absorbance was determined at 260 nm using UV spectrophotometer (V-530, Double beam Jasco, Tokyo, Japan) after appropriate dilution.

Particle size measurement

The particle size analysis of spray dried product was performed by laser scattering technique using Malvern Hydro 2000SM particle size analyzer (Malvern Instruments Ltd, Worcestershire, UK). Mean particle diameter in solid form and in liquid dispersion were calculated for each sample.

Polarized light microscopy

TDF loaded LCP (300 mg) was hydrated using phosphate buffer (5 mL pH 6.8) maintained at 37 ± 0.5 °C for 10 h. The hydrated samples were examined at each hour under polarized light microscope (Nikon, Eclipse E 600, Nikon Instech Co., Sendai, Japan) using λ ¼ compensator under 40× magnification to identify the type of mesophase formed. The photomicrographs of samples were taken

Table 1
Particle size, % yield, and drug content data of batches of TDF loaded LCP prepared using factorial design approach.

Batch	Lactose monohydrate (g)	Pluronic F127 (mg)	% Yield	Particle size (μm)	Drug content (mg/10 mg powder)
B1	1.5	100	40.23 ± 1.5	275.54 ± 3.46	1.43 ± 0.16
B2	1.5	60	52.13 ± 1.02	284.14 ± 2.68	2.98 ± 0.2
B3	1.5	20	42.58 ± 1.12	302.45 ± 2.19	2.58 ± 0.22
B4	1	100	36.03 ± 2.31	100.12 ± 4.65	2.89 ± 0.46
B5	1	60	49.37 ± 2.45	98.04 ± 1.54	3.68 ± 0.54
B6	1	20	39.4 ± 2.19	144.55 ± 3.89	2.6 ± 0.43
B7	0.5	100	12.64 ± 3.65	457.54 ± 1.36	0.98 ± 0.21
B8	0.5	60	13.42 ± 2.99	498.09 ± 1.27	1.14 ± 0.26
B9	0.5	20	11.52 ± 3.01	472.35 ± 1.94	0.87 ± 0.23

at room temperature during hydration at each hour (up to 10 h) and finally at 24 h to reveal the phase changes [26].

Small angle X-ray scattering (SAXS)

Bruker Nanostar (Massachusetts, United States) with rotating Cu anode and pinhole geometry with a copper Kα radiation of wavelength 1.54 Å was used to confirm the type of mesophase formed by the hydrated samples of TDF loaded LCP. A potential difference of 45 kV with anode having 100 mA current was used during the measurement. Hydrated sample of TDF loaded LCP was taken in a quartz capillary of 2 mm diameter and 10 μm wall thickness. Scattering from empty capillary was used as a background, which was subtracted, so as to obtain the sample absorption. Bruker Peltier heating cooling unit was used to maintain the temperature (25 ± 0.5 °C). The data was collected using HISTAR gas-filled multiwire detector [20].

Scanning electron microscopy (SEM)

SEM analysis of prepared TDF loaded LCP was performed to investigate its morphological characteristics. Samples were mounted on a double faced adhesive tape and sputtered with thin gold-palladium layer using sputter coater unit (VG Microtech, Uckfield, UK). Surface topography was analyzed using a Jeol JSM 6360 scanning electron microscope (SEM Jeol, Tokyo, Japan) operated at an acceleration voltage of 10 kV.

Fourier Transform Infrared Spectroscopy (FTIR)

FTIR spectra of TDF alone, Lactose, PF127, and GMO and TDF loaded LCP were recorded after appropriate background subtraction using FTIR spectrometer (Jasco FT/IR 4100, Oklahoma, USA) equipped with a diffuse reflectance accessory (Jasco PS 4000). Approximately, 2–3 mg sample was mixed with dry potassium bromide (40–50 mg) and the mixture was placed in the sample holder assembly of the equipment. The scanning of sample was performed in the range of 4000–400 cm^{-1}.

Differential Scanning Calorimetry (DSC)

Thermal behavior of TDF, GMO, Lactose, PF127, and TDF loaded LCP was analyzed using differential scanning calorimeter (Mettler Toledo, DSC 821^e, Greifensee, Switzerland). Each sample (approx. 5 mg) was placed in 40 μL aluminum pan and sealed hermetically. The sealed pans were subjected to heating at a rate of 10 °C/min over a temperature range 20–200 °C. Inert atmosphere was maintained during the whole heating cycle by purging nitrogen gas at a flow rate of 50 mL/min. Aluminum oxide was used as a standard reference material to calibrate the temperature and energy scale of DSC instrument.

Powder X-Ray Diffraction (PXRD)

The crystallinity of TDF and TDF loaded LCP was determined using X-ray diffractometer (PW 1729; Philips, Almelo, Netherlands). The samples were irradiated with Cu Kα radiation (1.542 Å) between 5 and 50° 2θ with a scan speed of 0.2 s/step and a step size of 0.0388°.

In- vitro drug release study

Drug release study of TDF loaded LCP and TDF alone was carried out using dynamic dialysis method [29]. LCP equivalent to 10 mg TDF was dispersed in water. The resulting suspension was poured in the pretreated dialysis bag (Ø 16 mm, MWCO 14,000 Da). Once sealed, the bag was placed in a beaker containing 200 mL phosphate buffer saline (PBS, pH 7.4) maintained at 37 °C with a continuous stirring at 100 rpm with the help of magnetic bead. The aliquots (3 mL) were aspirated at a predetermined time interval from the beaker and filtered through 0.45 μm membrane filter. The aliquots were analyzed spectrophotometrically at 260 nm after appropriate dilutions. Sink condition was maintained throughout the release test. Similar procedure was followed for TDF solution. The data were analyzed using PCP Disso V 3.0 software developed by Poona College of Pharmacy, Pune.

In vitro intestine membrane permeation studies

Fresh goat intestine obtained from the local slaughter house was cut along length to expose its internal surface. The tissue was rinsed and stored in cold PBS (pH 7.4) at 5 °C pending use. Franz diffusion cells having a diffusional surface area of 3.14 cm^2 and 20 mL receptor cell volume were used in the permeation study. The receptor compartment was filled with PBS (pH 7.4) stirred at constant speed to mix the contents. The outer side of the intestine was in contact with the receptor compartment fluid and equilibrated for 1 h to attain 37 ± 0.5 °C temperature. Aqueous dispersion of LCP (equivalent to 10 mg of TDF) was placed in the donor compartment. Aliquots of 2 mL were aspirated from receptor compartment at pre-determined time interval for 12 h. Sink conditions were maintained throughout the study. The aliquots were filtered and analyzed spectrophotometrically at 260 nm for TDF content. Similar procedure was fallowed for TDF solution.

Ex vivo permeation study

Non-everted intestinal sac method

The drug release and permeation from liquid crystal precursor using non-everted sac method was assessed at two conditions; (1) In the absence of digestive enzyme and (2) in the presence of digestive enzyme.

Drug permeation study in the absence of digestive enzyme

The non-everted sac experiments were performed based on the methods described elsewhere [27,28]. A small portion (5 ± 0.2 cm length) of fresh goat intestine was washed with ice cold normal oxygenated Krebs-Ringer phosphate buffer saline solution (pH 7.4) using a syringe equipped with blunt end. Each sac was tied at one end and filled with TDF loaded LCP dispersion (equivalent to 10 mg of TDF) prepared in 5 mL mixture of Krebs-Ringer buffer saline and isopropyl alcohol (7:3, *v/v*) via blunt needle in the muco-

sal compartment. The sac was sealed by tying the other end. Each non-everted intestinal sac was placed in 250 mL glass beaker containing 200 mL mixture of Krebs-Ringer Phosphate buffer saline solution (pH 7.4) and isopropyl alcohol (7:3, *v/v*) maintained at 37 °C with a constant stirring at 100 rpm. The experiment was performed under continuous aeration using laboratory aerator (10–15 bubbles/min). Samples (3 mL) were collected from the beaker (serosal compartment) at a predetermined time intervals for a period of 10 h and replaced with fresh medium. After filtration, the samples were scanned at 260 nm using UV spectrophotometer to determine TDF content. Similar procedure was used for TDF solution. *The study protocol was approved by Animal Ethics Committee of Bharati Vidyappeth University, Poona College of Pharmacy, Pune (Approval No. CPCSEA/7/2013).*

Drug permeation study in the presence of digestive enzyme

The TDF release experiments were performed in presence of digestive enzyme (pancreatic lipase) to assess its effect on TDF release and permeation across mucosa from lipoidal liquid crystal systems as these systems are prone to lipolysis by pancreatic lipase enzyme. Similar procedure as described in previous section was used with a slight change in dispersion medium. The dispersion medium inside the sac consisted of 3 mL mixture of Krebs-Ringer buffer saline: isopropyl alcohol (7:3, *v/v*) and 2 mL of pancreatic extract [29].

Calculation of apparent permeation coefficient

The permeability of TDF from the formulation was obtained by plotting a graph of cumulative TDF permeated through non-everted intestinal sac versus time (min). Permeation flux (F, μg/mL) was estimated from the graph (slope) after linear regression [29]. The apparent permeation coefficient (P_{app} cm/min) was calculated according to Eq. (1).

$$\mathbf{P_{app} = F/SA\ X\ C_0} \quad (1)$$

$$\mathbf{SA = 2\pi rh}$$

where SA is the surface area of the barrier membrane (cm^2); C_0 is the initial drug concentration (μg/mL) in the mucosal compartment, r is the intestinal segment mean radius (0.5 cm), and h is length of intestinal segment (5 cm).

Everted intestinal sac method

The TDF release and permeation from TDF loaded LCP in absence and presence of digestive enzyme was determined by everted sac method. A narrow glass rod was inserted into one end of the intestine. A ligature was tied over the thickened part of the glass rod and intestine sac was everted gently by pushing the rod through the whole length of the intestine. The glass rod was removed and the intestine was placed in a glucose-saline solution at room temperature until used. The procedure for TDF release study in everted sac was similar to that described for non-everted sac method.

Stability study

Stability studies were conducted to test the physical and chemical stability of the spray dried TDF loaded LCP. ICH Q1A (R2) guidelines with slight modification in the storage period were followed testing the stability of spray dried samples. Sample (2 g) was stored at different temperature conditions of 4 ± 3 °C, 25 °C/60% RH, 40 °C/75% RH, and room temperature for 90 days. The physical stability including appearance, moisture content, particle, size and drug content was analyzed.

Statistical analysis

The data obtained from various studies was statistical analyzed using one way ANOVA followed by posthoc test. All the measurements were performed in triplicate to ensure the accuracy of the data.

Results

The ability of GMO to transform into stable cubic liquid crystalline phase has been utilized in the present study. Bioadhesive property of GMO was enhanced by using PF127 so as to prolong the contact between cubic phase and intestinal mucous membrane. Lactose monohydrate, used as adsorbent, dissolved immediately when the LCP come into contact with the GI fluid (water) transforming into cubic phase.

Influence on independent variables

Drug content

The regression equation for drug content using factorial design approach is depicted below (Eq. (2)).

$$\text{Drug content} = 3.42 + 0.83X_1 + 0.042X_2 - 0.067X_1X_2 - 1.23X_1^2 - 0.54X_2^2 \quad R^2 = 0.9315 \quad (2)$$

The drug content increased with increase in the amount of lactose and PF127. However as revealed by the coefficients of the variables, the amount of lactose had a drastic effect on drug content as compared to PF127 (Fig. 1A).

Particle size

The regression equation for particle size using factorial design approach is given below (Eq. (3)).

$$\text{Particle Size} = 115.13 - 94.31X_1 - 14.36X_2 - 3.03X_1X_2 + 267.45X_1^2 - 1.33X_2^2 \quad R^2 = 0.9823 \quad (3)$$

Particle size of all the batches decreased with increase in the amount of lactose. Lactose was used as an adsorbent for GMO and TDF. It also helps in obtaining spherical particles. Similarly, increase in the amount of PF127 showed reduction in the particle size (Fig. 1B). The results of particle size, drug content, and % yield suggested batch B5 as optimized batch.

The TDF content of optimized TDF loaded LCP batch was 36.82 ± 0.542%w/w with a particle size of 98.042 ± 1.54 μm in solid state and 74.5 ± 0.068 nm upon hydration, indicating formation of nanoparticles. The total yield of the optimized TDF loaded LCP was 43.41%.

Plane polarized light (PPL) microscopy

PPL microscopy can identify the type of mesophase formed upon hydration of liquid crystalline system [30,31]. PPL images of hydrated TDF loaded LCP samples revealed complete isotropy when analyzed at different time intervals including 24 h (Fig. 2).

Small angle X-ray scattering (SAXS)

Cubic phase microstructure formed by TDF loaded LCP showed a double diamond type of geometry when analyzed by SAXS. The diffraction peaks of nanoparticles were in the ratio of $\sqrt{2}:\sqrt{3}:\sqrt{4}:\sqrt{6}:\sqrt{8}:\sqrt{9}$, confirming the formation of cubosomes upon hydration of the spray dried powder (Fig. 3A) [20].

Scanning electron microscopy (SEM)

Scanning electron microscopy of samples can elucidate the morphological characteristics of TDF. SEM image of TDF alone

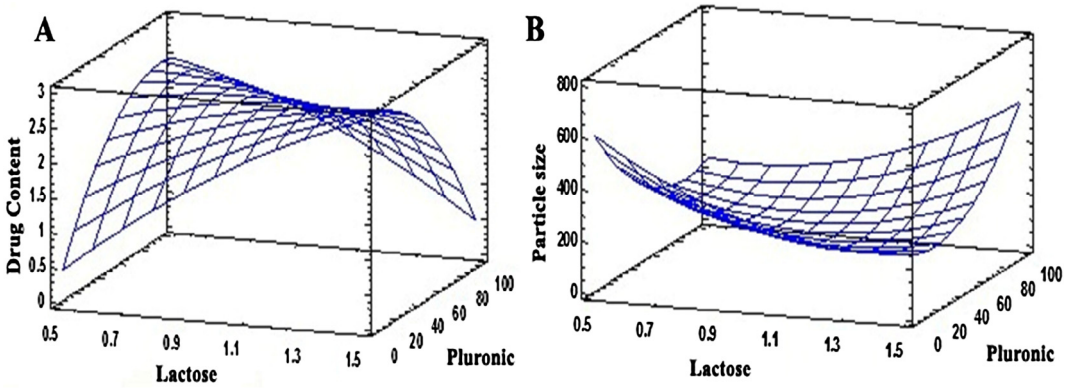

Fig. 1. Effect of independent variables on (A) Drug content and (B) Particle size.

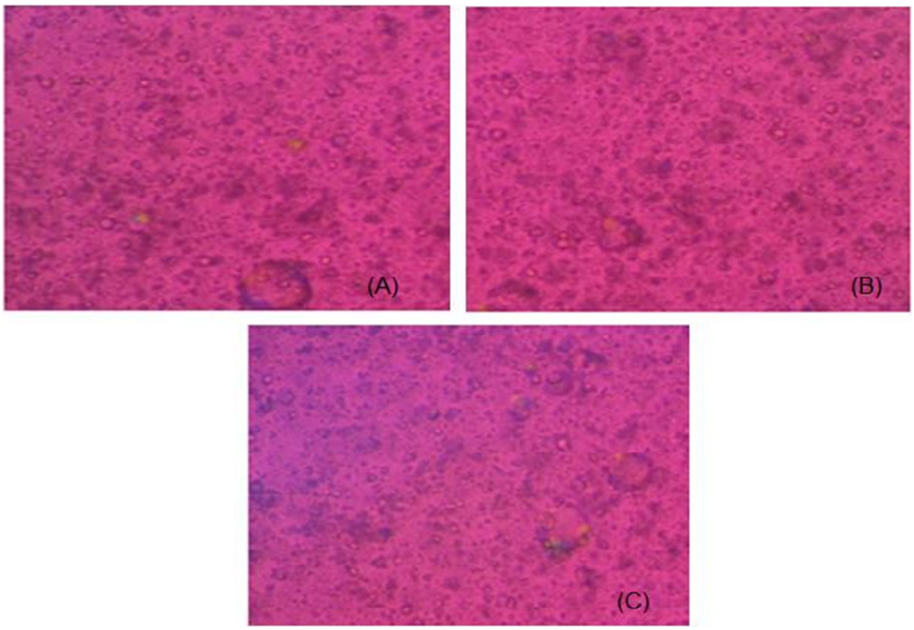

Fig. 2. Polarized light microscopy images of TDF loaded LCP after (A) 1 h, (B) 10 h, and (C) 24 h hydration.

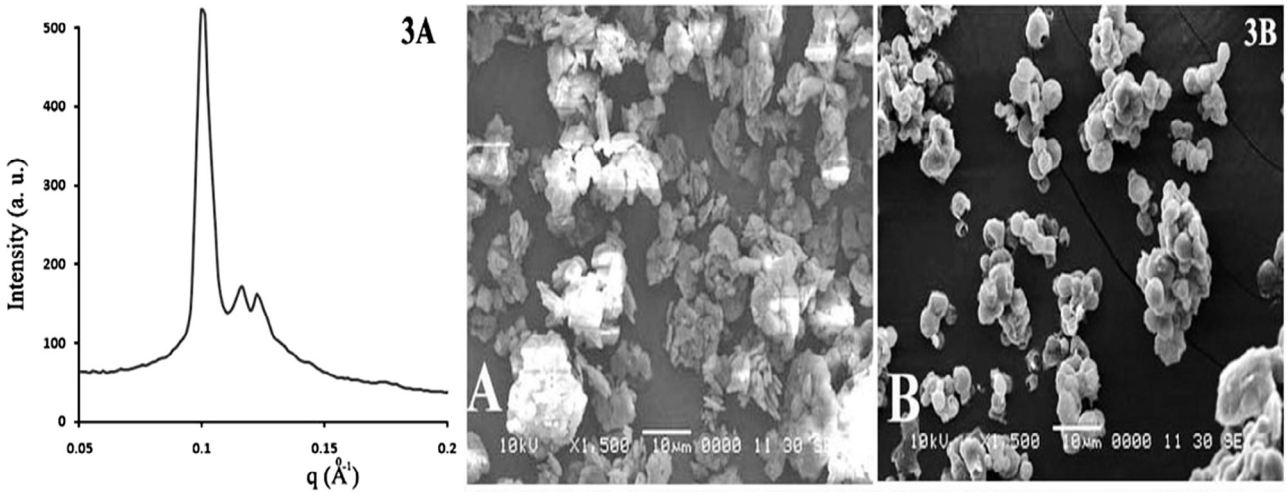

Fig. 3. (A) SAXS pattern of hydrated sample of TDF loaded LCP. (B) SEM image of (A) TDF alone and (B) Spray dried TDF loaded LCP.

showed irregular shaped clusters of microparticles (Fig. 3B). However, SEM photograph of TDF loaded LCP showed aggregation of spherical particles with smooth surface texture.

Fourier Transform Infrared Spectroscopy (FTIR)

FTIR spectra helps in identifying the interactions between the drug and carrier at molecular level. FTIR spectra of TDF, GMO, Lactose, PF127, and TDF loaded LCP are shown in Fig. 4A. TDF showed characteristic peaks at 3322.75, 2985.27, 1736, 1689, 1267.97, 1103.88, 727.996, 681.22, and 627.77 cm^{-1} [32]. FTIR peaks at 1689 and 1736 cm^{-1} represented C═O stretching from fumarate portion of TDF, while the peak at 3322.75 cm^{-1} represented NH_2 stretching vibration. IR peak at 1267.97 and 1103.88 cm^{-1} were due to C═C stretching in aromatic ring and C—O group/CH_2OH stretching, respectively. Peaks around 2985.27, 727.996 and 627.77 cm^{-1} corresponded to CH aliphatic stretching, out of plane CH_2 bending and CH bending, respectively. A peak at 681.22 cm^{-1} suggested the presence of aromatic ring with out plane bending. The IR spectra of GMO (Fig. 4A) showed characteristic peak at 3400 cm^{-1} due to O—H stretching vibration. The CH_2 stretching and presence of ester bond, C═O was confirmed by the peaks at 2937.45 and 1730.22 cm^{-1}.

FTIR spectrum of lactose monohydrate showed peak at 3530.06 cm^{-1} representing vibration of O—H bond associated with the water of crystallization. However, peaks at 3386.39 and 3343.22 cm^{-1} revealed the presence of O—H stretching, indicating intermolecular H-bond formation. A triplicate at 2977.21, 2934.16, and 2900.41 cm^{-1} represented C—H stretch due to methylene group present in lactose monohydrate. Peaks in the range of 1425.14 to 1295.94 cm^{-1}, suggested in plane bending vibration of O—H group. The peaks around 1260.24 to 1000.95 cm^{-1} were associated with the stretching vibrations due to C—O in fact C—O-C bonds [33]. IR spectra of PF127 showed peaks at 2974.66, 1343.18, and 1060.66 cm^{-1} corresponding to C—H aliphatic stretch, in plane O—H bond, and C—O stretch, respectively [34]. The characteristic peaks associated with TDF, GMO, lactose monohydrate, and PF127 retained in the FTIR spectrum of TDF loaded LCP.

Differential Scanning Calorimetry (DSC)

DSC thermograms of TDF alone, GMO, PF127, lactose monohydrate, and TDF loaded LCP are shown in Fig. 4B. TDF alone showed characteristic endothermic peak in the range of 111–115 °C, indicating its melting point, whereas GMO showed melting endotherm at about 39 °C [35]. Additionally, PF127 showed melting endotherm at 56 °C, whereas endotherm at 143 °C for lactose monohydrate suggested loss of water of crystallization by lactose. The melting point of lactose was 215 °C. However, DSC thermogram of TDF loaded LCP showed endotherms at 45 and 143 °C.

Powder X-Ray Diffraction (PXRD)

Powder X-ray diffractograms recorded for TDF alone and TDF loaded LCP so as to investigate the crystallinity of TDF upon its transformation into LCP (Fig. 5). TDF alone showed characteristic diffraction peaks at 2θ values of 5°, 10.3°, 10.6°, 18.3°, 20°, 22°, 24.1°, 25.1°, 25.5°, and 30.2°. However, PXRD of TDF loaded LCP did not show sharp X-ray diffraction peaks.

In vitro drug release

The dissolution profile of TDF solution showed nearly 100% TDF release in 2 h. However, the dissolution profile of TDF loaded LCP showed biphasic behavior consisting of initial burst release followed by a slow drug release (Fig. 6A). The investigation of drug release kinetics of TDF loaded LCP showed zero order kinetics (R^2 = 0.998) releasing around 99% of TDF in a period of 10 h. The drug release studies were also carried out at different pH to investigate the effect of pH on release kinetics of the prepared TDF loaded LCP and in turn to evaluate its stability at these pH conditions. TDF release from prepared precursor showed similar pattern with zero order kinetics at different pH conditions, including 1.2, 4.5, 6.8 and 7.4 (Data not shown).

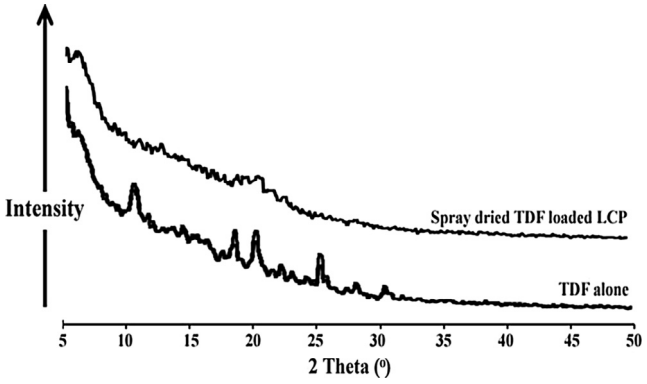

Fig. 5. PXRD patterns of TDF alone and spray dried TDF loaded LCP.

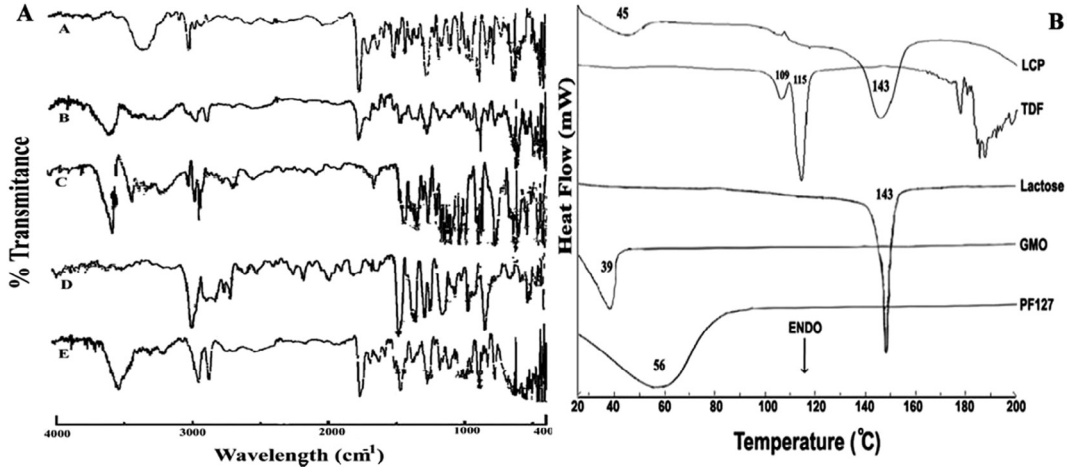

Fig. 4. (A) FTIR spectra of (A) TDF, (B) TDF loaded LCP, (C) Lactose monohydrate, (D) PF127 and (E) GMO. (B) DSC thermogram of PF127, GMO, Lactose, TDF and LCP.

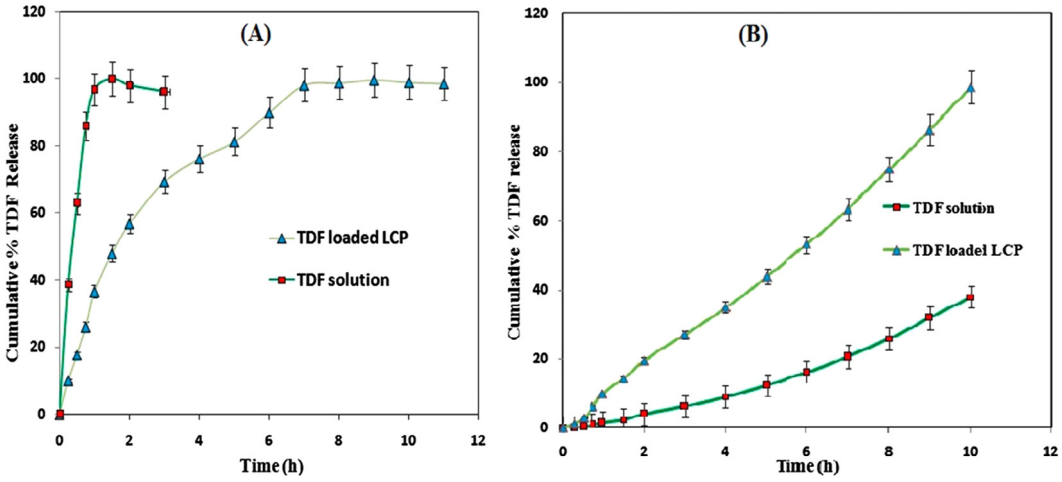

Fig. 6. (A) Comparison of *in vitro* % TDF release from TDF solution and TDF loaded LCP. (B) Comparison of *in vitro* permeation of TDF through goat intestine membrane (n = 3).

In vitro intestine permeation study

TDF permeation across goat intestinal membrane performed for TDF loaded LCP and TDF solution (Fig. 6B). The percent cumulative drug release at the end of 10 h was found to be 98.54 ± 1% and 37.98 ± 1.5% for TDF loaded LCP and TDF solution, respectively. TDF loaded LCP showed controlled TDF release with increased TDF permeation over a period of 10 h. The mathematical treatment of data showed multiple drug release kinetics for TDF loaded LCP. The cubic liquid crystalline phase formed by the precursor followed zero order kinetics along with Korsmeyer-peppas model. Zero order model (R^2 = 0.994) suggests that drug release from formulation was independent initial concentration of drug available for release. Korsmeyer-peppas model (R^2 = 0.991) suggested that TDF release followed non-fickian drug transport (n = 0.631). Moreover, the average permeation flux values for TDF alone and TDF loaded LCP were found to be 0.04 ± 0.02 and 0.21 ± 0.12%/h, respectively.

Ex vivo permeation study

Ex vivo permeation study by non-everted intestine sac method

It is known that to estimate the appropriate and logical drug permeation, the study should be performed using a biological membrane. Thus in the present study, we used goat intestine for *ex vivo* TDF permeation study. The percent TDF release across goat intestine from TDF solution in presence and absence of digestive enzymes was only 26 ± 2% at the end of 10 h (Fig. 7A). Thus, the presence of digestive enzymes did not alter the percent TDF release. However, TDF loaded LCP showed 86 ± 1.5% of TDF release in the absence of digestive enzymes extract at the end of 6 h. Additionally, TDF release for LCP in presence of digestive enzymes was 98 ± 1% at the end of 6 h. Therefore, the prepared powder precursor showed a controlled and increased drug release over a period of 10 h. The mathematical treatment of data showed that the TDF release from prepared powder precursor followed zero order kinetics (R^2 = 0.990).

The TDF permeation flux and permeability coefficient values for TDF solution were approximately the same ($P > 0.05$) in presence and absence of digestive enzymes extract, respectively. The permeation flux for TDF from LCP was found to be 17.45 ± 1.34 and 21.86 ± 1.01%/h with a permeability coefficient of 11.11 ± 2.19 and 13.91 ± 2.31 in absence and presence of digestive enzymes, respectively, which were found to be significantly higher when compared to the flux values from TDF solution ($P < 0.05$). The low permeation flux for TDF was attributed to its inherent low permeability (Table 2).

Ex vivo permeation everted intestine sac method

The effect of viscous mucous layer lining on TDF permeation was tested using everted goat intestine. The percent TDF release from TDF solution in presence and absence of digestive enzymes was found to be 31 ± 2% at the end of 10 h (Fig. 7B). However, TDF loaded LCP showed 79 ± 1.5% TDF release when tested in absence of digestive enzymes at the end of 10 h, which is signifi-

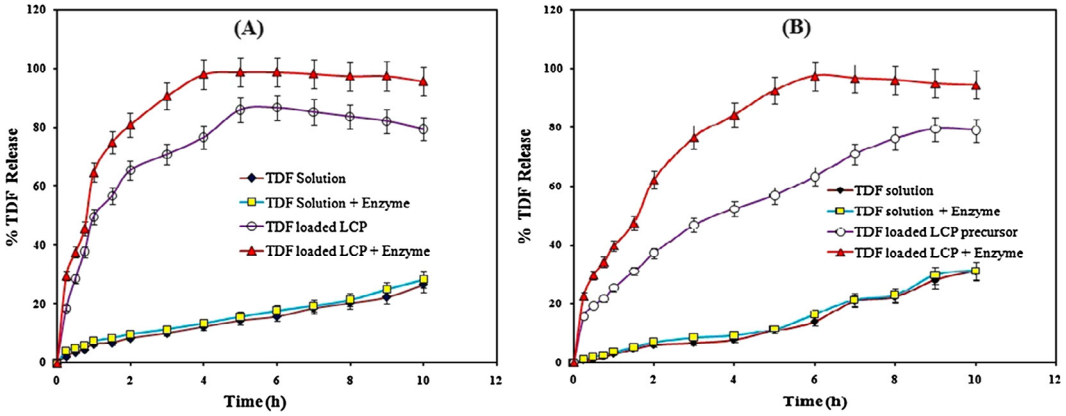

Fig. 7. Comparison of *ex vivo* permeation of TDF through (A) non-everted (B) everted goat intestine membrane (n = 3).

Table 2
Permeation flux (%/h) values of TDF from non-everted and everted intestine sac permeation study.

Parameter	TDF permeation from non-everted intestine sac				TDF permeation from everted intestine sac			
	Absence of enzyme		Presence of enzyme		Absence of enzyme		Presence of enzyme	
	TDF solution	TDF loaded LCP	TDF solution	TDF loaded LCP	TDF solution	TDF loaded LCP	TDF solution	TDF loaded LCP
Permeation flux (%/h)	3.41 ± 0.21	17.45 ± 1.34**	3.62 ± 0.37 ns	21.86 ± 1.0**	3.07 ± 1.03	11.94 ± 1.28**	3.70 ± 1.34 ns	16.86 ± 1.34**
Apparent permeation coefficient (cm/h)^2	2.17 ± 1.04	11.11 ± 2.2**	2.3 ± 1.11 ns	13.91 ± 2.31**	1.95 ± 1.27	7.6 ± 1.57**	2.35 ± 1.18 ns	10.73 ± 1.84**

Mean ± SD. Data analyzed by one way ANOVA followed by posthoc Dunnett's test, with *$P < 0.05$ considered significant, **$P < 0.01$, ns – nonsignificant, n = 3.

cantly less ($P < 0.05$) than percent TDF released in non-everted sac study under the similar set of conditions. Surprisingly, powder precursor showed 97 ± 1% TDF release when tested in the presence of digestive enzyme extract at the end of 6 h, which is comparable to TDF release from non-everted sac study under similar set of conditions. The cubic phase formed by the precursor showed a controlled and increased TDF release over a period of 10 h. The best fit model for *ex vivo* everted sac permeation study involving formation of cubic phase followed zero order kinetics along with Korsmeyer-Peppas model. Zero order model ($R^2 = 0.996$), suggested independence of initial TDF concentration on TDF release, whereas part of TDF released following Fick's law of diffusion as suggested by Korsmeyer-Peppas model ($R^2 = 0.992$) with a 'n' value of 0.477.

The permeation flux and permeability coefficient values for TDF permeation through TDF solution in presence and absence of digestive enzyme extract were found comparable, confirming the absence of any detrimental effect of digestive enzyme extract on TDF. The permeation flux for TDF from LCP was found to be 11.94 ± 1.28 and 16.86 ± 1.34%/h with a permeability coefficient of 7.6 ± 1.57 and 10.73 ± 1.84 in absence and presence of digestive enzymes, respectively (Table 2).

Stability study

The utility of prepared formulation depends on its long term stability, thus stability test was designed for prepared LCP for a period of 90 days. Particle size analysis of prepared LCP did not show significant alterations when stored at different temperatures and humidity conditions such as 4 ± 3 °C, 25 °C/60% RH, 40 °C/75% RH, and room temperature, indicating physical stability of prepared LCP ($P > 0.05$). Similarly, TDF content studies of prepared powder precursors revealed insignificant changes in the percent TDF content when stored at 4, 25, and 40 °C for 90 days, indicating chemical stability of the precursors at refrigerated, room, and accelerated temperature conditions (Table 3).

Discussion

It is known that among the three liquid crystalline phases (lamellar, cubic, and hexagonal), both lamellar and hexagonal show birefringence. Thus, the absence of birefringence in the hydrated samples of the prepared precursors indicated transformation into stable cubic mesophase. GMO alone when hydrated in water at room temperature forms a cubic phase [30,31]. Therefore, the results of PPL microscopy study suggested that the additives used in the LCP do not alter the mesophase formed by GMO alone as reported previously. Additionally, the observations of PPL microscopy were confirmed using SAXS analysis of the hydrated TDF loaded LCP sample. Cubic mesophases formed by the liquid crystals can be of three types viz. primitive (double diamond or simple cubic), face-centered, and body centered cubic phase. GMO has been reported to form primitive cubic phase in water that could be readily confirmed from SAXS pattern [20]. The analysis of SAXS pattern of hydrated TDF loaded liquid crystals confirmed the formation of cubic phase with double diamond architecture. Further, the spherical spray dried samples of TDF loaded LCP had a smooth surface, which could be attributed to the presence of lipidic GMO on the surface of particles. The absence of TDF particles alone in the SEM of TDF loaded LCP suggested their entrapment into GMO/PF127 matrix. In order to assess whether the loading of TDF into GMO/PF127 matrix involves any chemical interaction, FTIR studies were carried out. The characteristic peaks associated with TDF, GMO, lactose monohydrate, and PF127 were retained in the FTIR spectrum of TDF loaded LCP, suggesting the absence any chemical interaction between these components and confirming the physical entrapment of TDF in GMO/PF127 matrix.

DSC studies were carried out to investigate the readings of FTIR studies. DSC thermogram of TDF loaded LCP did not show melting endotherm corresponding to the melting of TDF. Such behavior can be attributed to the monotectic behavior of the system [36]. It is well reported in the literature that if the system contains components having low melting point, other components may get solubilized in the molten component depending on their polarity. Thus, TDF might have been solubilized in the molten amphiphillic GMO chains and in turn did not show melting behavior in the thermogram. Additionally, the second endotherm observed at 143 °C could be attributed to the loss of water from lactose monohydrate as reported earlier in the literature [33]. The results of PXRD were also in agreement with the readings of FTIR, SEM, and DSC studies, wherein TDF loaded LCP did not show characteristics sharp PXRD peaks for TDF. Virtual disappearance of sharp peaks of TDF in TDF loaded LCP suggested molecular entrapment or dispersion in

Table 3
Stability study data TDF loaded LCP.

Days	4 °C (Refrigerated condition)		25 °C (Room temperature)		40 °C (Accelerated condition)	
	Particle size (μm) ± SD	% TDF content ± SD	Particle size (μm) ± SD	% TDF content ± SD	Particle size (μm) ± SD	% TDF content ± SD
0	98.04 ± 1.54	98 ± 1.03	98.04 ± 1.54	98 ± 1.03	98.04 ± 1.54	98 ± 1.03
30	97.34 ± 1.98 ns	97.34 ± 0.98 ns	98.12 ± 1.97 ns	97.25 ± 1.27 ns	100.99 ± 2.03 ns	98.09 ± 1.12 ns
60	98.54 ± 1.68 ns	97.54 ± 1.12 ns	99.52 ± 1.67 ns	98.02 ± 1.00 ns	101.24 ± 2.45 ns	98.44 ± 1.21 ns
90	99.37 ± 1.52 ns	96.97 ± 1.01 ns	99.23 ± 1.45 ns	97.21 ± 0.5 ns	104.59 ± 2.94 ns	97.59 ± 1.27 ns

Mean ± SD, Tukey's multiple comparison test with *$P < 0.05$ considered significant, ns – nonsignificant, n = 3.

the lipophilic environment of GMO/PF127 matrix. Yet, another reason for disappearance of characteristic PXRD peaks of TDF could be associated with its conversion from crystalline to amorphous form [36].

In vitro drug release studies were carried out to analyze the drug release kinetics of the prepared precursors that was compared to TDF solution. The rapid release of TDF from TDF solution was obvious owing to its hydrophilic nature. However, the TDF loaded LCP showed biphasic drug release characteristics with a controlled release of TDF as suggested by the model fitting data. It is understood that the controlled release of TDF from the formulation is associated with the highly viscous matrix produced by the cubic phase liquid crystals as highlighted earlier. The initial burst release of TDF from the formulation can be attributed to the presence of free TDF in the external phase and adsorbed on the surface of particles, while the controlled release may be due to TDF encapsulated within the cubic phase of GMO. The release pattern of formulated liquid crystalline system indicated that using this delivery system, a loading dose of around 40% of TDF could be made available within 1 h of its administration, while the remaining would support the maintenance dose for a considerable duration and in turn may prevent excessive fluctuations in the drug plasma level. It is well reported in the literature that the cubic phase formed by GMO remains stable at all gastrointestinal pH conditions [17]. Thus observation of similar drug release characteristic from the formulation at different pH conditions was in accordance with the literature.

It is put onto the records that GMO having polar head and nonpolar carbon chain with a low melting point increases permeability of membrane by disordering intercellular lipid. Further, the interaction between polar head of phospholipid and a hydroxyl group of GMO has been identified as a possible mechanism for permeation enhancement of drugs by transdermal route [37,38]. It is believed that similar mechanisms might have been responsible for enhancing permeation flux and coefficient values of TDF by oral route along with bioadhesive nature of GMO increasing residence time in GI tract. Moreover, it is well reported in the literature that GMO is digested to oleic acid and glycerol by the pancreatic lipase [39]. Further, oleic acid generated upon digestion of GMO has been used as a permeation enhancer in many formulations. The reports state that oleic acid molecules distort the lipid bilayer of cells through formation of separate phases, which in turn creates permeability defects in the cell membrane increasing the permeability of drug molecules [40]. Thus *in vivo* generation of oleic acid from the prepared TDF loaded LCP might have increased the permeation of TDF when the studies were carried out in presence of digestive enzymes. The proposed hypothesis was verified as the TDF release and permeation flux values were similar ($P > 0.05$) for TDF solution when tested in presence of digestive enzymes for both everted and non-everted intestine sac. Additionally, it also confirmed that the digestive enzymes do not have any detrimental effect on TDF.

The permeation studies were also performed on everted goat intestine in order to determine the effect of viscous mucous layer on TDF permeation. The comparison of permeation studies of TDF across everted and non-everted intestinal sacs showed that the flux values were less for everted intestinal sac. The high TDF permeation flux values associated with non-everted sac may be attributed to the presence of viscous mucous layer lining facilitating TDF permeation due to prolonged contact between viscous TDF loaded cubic phase formulation and gastrointestinal luminal membrane along with penetration enhancer oleic acid generated upon digestion of GMO. Thus to conclude, permeation of TDF across intestine was governed by viscous mucus layer lining and the cubic phase formed by the prepared powder precursor.

Conclusions

The current work demonstrates utility of spray dried cubic phase LCP of GMO-Pluronic F127 in permeation enhancement of TDF when given orally. The results of present study indicate possibility of improvement in oral bioavailability of TDF when formulated as cubic phase LCP owing to its permeation enhancing activity. Formulation of stable LCP can serve as an alternative for designing oral delivery system for drugs with low permeability.

Acknowledgements

Authors CLK and VP are thankful to Danisco India Pvt. Ltd for their co-operation and gift sample of Glyceryl monooleate (RYLO MG 19 Pharma). Authors are also thankful to Emcure Pharmaceuticals, Pune, India for gifting sample of Tenofovir disoproxil fumarate (TDF).

Conflict of Interest

The authors have declared no conflict of interest.

Compliance with Ethics Requirements

All Institutional and National Guidelines for the care and use of animals were followed. Goat intestine was used for permeation study which was brought from local slaughter house.

References

[1] Van Hoogdalem E, De Boer A, Breimer D. Intestinal drug absorption enhancement: an overview. Pharmacol Therapeut 1989;44:407–43.
[2] Pabla D, Akhlaghi F, Zia H. Intestinal permeability enhancement of levothyroxine sodium by straight chain fatty acids studied in MDCK epithelial cell line. Eur J Pharm Sci 2010;40(5):466–72.
[3] Chen L, Tan F, Wang J, Liu F. Microemulsion: a novel transdermal delivery system to facilitate skin penetration of indomethacin. Pharmazie 2012;67(4):319–23.
[4] Sakeena M, Elrashid S, Muthanna F, Ghassan Z, Kanakal M, Laila L, et al. Effect of limonene on permeation enhancement of ketoprofen in palm oil esters nanoemulsion. J Oleo Sci 2010;59(7):395–400.
[5] Yavuz B, Bilensoy E, Vural I, Sumnu M. Alternative oral exemestane formulation: improved dissolution and permeation. Int J Pharm 2010;398:137–45.
[6] Thanou M, Verhoef J, Junginger H. Oral drug absorption enhancement by chitosan and its derivatives. Adv Drug Deliv Rev 2001;52:117–26.
[7] Chitneni M, Peh K, Darwis Y, Abdulkarim M, Abdullah G, Qureshi M. Intestinal permeability studies of sulpiride incorporated into self-micro emulsifying drug delivery system (SMEDDS). Pak J Pharm Sci 2011;24:113–21.
[8] Shen G, Xing R, Zhang N, Chen C, Ma G, Yan X. Interfacial cohesion and assembly of bioadhesive molecules for design of long-term stable hydrophobic nanodrugs toward effective anticancer therapy. ACS Nano 2016;10(6):5720–9.
[9] Lim D, Jeong W, Kim N, Lim J, Lee S, Shim W, et al. Effect of the glyceryl monooleate-based lyotropic phases on skin permeation using *in vitro* diffusion and skin imaging. AJPS 2014;9(6):324–9.
[10] Wu X, Todo H, Sugibayashi K. Enhancement of skin permeation of high molecular compounds by a combination of microneedle pretreatment and iontophoresis. J Control Release 2007;118(2):189–95.
[11] Van Der Bijl P, Basson E, Van Eyk A, Seifart H. Effect of ultrasound on transdermal permeation of diclofenac. Eur J Inflamm 2006;4(2):109–16.
[12] Nalluri B, Anusha S, Bramhini S, Amulya J, Sultana A, Teja C, et al. *In vitro* skin permeation enhancement of sumatriptan by microneedle application. Curr Drug Deliv 2015;12(6):761–9.
[13] Han T, Das D. Potential of combined ultrasound and microneedles for enhanced transdermal drug permeation: a review. Eur J Pharm Biopharm 2015;89:312–28.
[14] Lee W, Shen S, Fang C, Zhuo R, Fang J. Topical delivery of methotrexate via skin pretreated with physical enhancement techniques: low-fluence erbium:YAG laser and electroporation. Laser Surg Med 2008;40(7):468–76.
[15] Kim J, Jang J, Lee J, Choi J, Park W, Bae I, et al. Enhanced topical delivery of small hydrophilic or lipophilic active agents and epidermal growth factor by fractional radiofrequency microporation. Pharm Res 2012;29(7):2017–29.
[16] Banga A. Microporation applications for enhancing drug delivery. Expert Opin Drug Del 2009;6(4):343–54.

[17] Kumar K, Shah M, Ketkar A, Mahadik K, Paradkar A. Effect of drug solubility and different excipients on floating behaviour and release from glyceryl monooleate matrices. Int J Pharm 2004;272:151–60.
[18] Norling T, Lading P, Engström S, Larsson K, Krog N, Nissen S. Formulation of a drug delivery system based on a mixture of monoglycerides and triglycerides for use in the treatment of periodontal disease. J Clin Periodontol 1992;19:687–92.
[19] Nielsen L, Schubert L, Hansen J. Bioadhesive drug delivery system, I: characterization of mucoadhesive properties of systems based on glyceryl monooleate and glyceryl monolinoleate. Eur J Pharm Sci 1998;6:231–9.
[20] Patil S, Venugopal E, Bhat S, Mahadik K, Paradkar A. Mapping ion-induced mesophasic transformation in lyotropic in situ gelling system and its correlation with pharmaceutical performance. Pharm Res 2013;30:1906–14.
[21] Spicer P, Small W, Lynch M, Burns J. Dry powder precursors of cubic liquid crystalline nanoparticles (cubosomes). J Nanopart Res 2002;4:297–311.
[22] Shah M, Paradkar A. Cubic liquid crystalline glyceryl monooleate matrices for oral delivery of enzyme. Int J Pharm 2005;294:161–71.
[23] Maheshwari M, Paradkar A, Yamamura S, Kadam S. Preparation and characterization of pluronic-colloidal silicon dioxide composite particles as liquid crystal precursor. AAPS PharmSciTech 2006;7(4):92.
[24] Shaikh M, Nikita D, Rajendra B. Permeability enhancement techniques for poorly permeable drugs: a review. J Appl Pharm Sci 2012;2(6):34–9.
[25] Patil S, Choudhary B, Rathore A, Roy K, Mahadik K. Enhanced oral bioavailability and anticancer activity of novel curcumin loaded mixed micelles in human lung cancer cells. Phytomedicine 2015;22:1103–11.
[26] Rosevear F. The microscopy of the liquid crystalline neat and middle phases of soaps and synthetic detergents. J Am Oil Chem Soc 1954;31:628–39.
[27] Freag M, Elnaggar Y, Abdallah O. Development of novel polymer-stabilized diosmin nanosuspensions: *in vitro* appraisal and *ex vivo* permeation. Int J Pharm 2013;454(1):462–71.
[28] Lassoued M, Khemiss F, Sfar S. Comparative study of two *in vitro* methods for assessing drug absorption: sartorius sm 16750 apparatus versus everted gut sac. J Pharm Pharm Sci 2011;14(1):117–27.
[29] Bothiraja C, Pawar A, Dama G, Joshi P, Shaikh K. Novel solvent free gelucire extract of Plumbago zeylanica using non-everted rat intestinal sac method for improved therapeutic efficacy of plumbagin. J Pharmacol Toxicol 2012;66(1):35–42.
[30] Patil S, Venugopal E, Bhat S, Mahadik K, Paradkar A. Probing influence of mesophasic transformation in self-emulsifying system: effect of Ion. Mol Pharm 2012;9:318–24.
[31] Patil S, Venugopal E, Bhat S, Mahadik K, Paradkar A. Microstructural elucidation of self-emulsifying system: effect of chemical structure. Pharm Res 2012;29:2180–8.
[32] Lee E, Smith D, Fanwick P, Byrn S. Characterization and anisotropic lattice expansion/contraction of polymorphs of tenofovir disoproxil fumarate. Cryst Growth Des 2010;10(5):2314–22.
[33] Patil S, Mahadik K, Paradkar A. Liquid crystalline phase as a probe for crystal engineering of lactose: carrier for pulmonary drug delivery. Eur J Pharm Sci 2015;68:43–50.
[34] Lin J, Chen J, Huang S, Ko J, Wang Y, Chen T, et al. Folic acid-Pluronic F127 magnetic nanoparticle clusters for combined targeting, diagnosis, and therapy applications. Biomaterials 2009;30(28):5114–24.
[35] Gomes E, Mussel W, Resende J, Fialho S, Barbosa J, Carignani E, et al. Characterization of tenofovir disoproxil fumarate and its behavior under heating. Cryst Growth Des 2015;15(4):1915–22.
[36] Vippagunta S, Maul K, Tallavajhala S, Grant D. Solid-state characterization of nifedipine solid dispersions. Int J Pharm 2002;236(1–2):111–23.
[37] Ogiso T, Iwaki M, Paku T. Effect of various enhancers on transdermal penetration of indomethacin and urea and relationship between penetration parameters and enhancement factors. J Pharm Sci 1995;84:482–8. Washington.
[38] Pereira G, Collett J, Garcia S, Thomazini J, Bentley M, et al. Glycerol monooleate/solvents systems for progesterone transdermal delivery: *in vitro* permeation and microscopic studies. Braz J Pharm Sci 2002;38:55–62.
[39] Kalepun S, Manthina M, Padavala V. Oral lipid-based drug delivery systems – an overview. APSB 2013;3(6):361–72.
[40] Trommer H, Neubert R. Overcoming the stratum corneum: the modulation of skin penetration. Skin Pharmacol Physi 2006;19:106–21.